NAVAL POSTGRADUATE SCHOOL
Monterey, California

THESIS

PHOTOCURRENT GENERATION FROM BASIC METALS,
UTILIZING A SHORT PULSED ArF EXCIMER LASER

by

Thomas J. Ringler

September 1987

Thesis Advisor: F. R. Buskirk

Approved for public release; distribution is unlimited.

SECURITY CLASSIFICATION OF THIS PAGE

REPORT DOCUMENTATION PAGE

1a REPORT SECURITY CLASSIFICATION UNCLASSIFIED	1b RESTRICTIVE MARKINGS
2a SECURITY CLASSIFICATION AUTHORITY	3 DISTRIBUTION/AVAILABILITY OF REPORT Approved for public release; distribution is unlimited.
2b DECLASSIFICATION/DOWNGRADING SCHEDULE	
4 PERFORMING ORGANIZATION REPORT NUMBER(S)	5 MONITORING ORGANIZATION REPORT NUMBER(S)
6a NAME OF PERFORMING ORGANIZATION Naval Postgraduate School	6b OFFICE SYMBOL (If applicable) 61
7a NAME OF MONITORING ORGANIZATION Naval Postgraduate School	
6c ADDRESS (City, State, and ZIP Code) Monterey, California 93943-5000	7b ADDRESS (City, State, and ZIP Code) Monterey, California 93943-5000
8a NAME OF FUNDING/SPONSORING ORGANIZATION	8b OFFICE SYMBOL (If applicable)
9 PROCUREMENT INSTRUMENT IDENTIFICATION NUMBER	
8c ADDRESS (City, State, and ZIP Code)	10 SOURCE OF FUNDING NUMBERS PROGRAM ELEMENT NO / PROJECT NO / TASK NO / WORK UNIT ACCESSION NO

11 TITLE (Include Security Classification)
PHOTOCURRENT GENERATION FROM BASIC METALS, UTILIZING A SHORT PULSED ArF EXCIMER LASER

12 PERSONAL AUTHOR(S)
Ringler, Thomas J.

13a TYPE OF REPORT	13b TIME COVERED	14 DATE OF REPORT (Year, Month, Day)	15 PAGE COUNT
Master's Thesis	FROM _____ TO _____	1987 September	61

16 SUPPLEMENTARY NOTATION

17 COSATI CODES			18 SUBJECT TERMS (Continue on reverse if necessary and identify by block number)
FIELD	GROUP	SUB-GROUP	Photoelectric Effect ArF Excimer Laser Photoemission Quantum Efficiencies for Metals

19 ABSTRACT (Continue on reverse if necessary and identify by block number)

An excimer laser used to produce "cold" photoelectrons from common metal surfaces offers an improvement over a standard heated (thermionic) cathode electron source. Photoelectrons accelerated across an anode cathode gap were observed under both space charge limited and emission limited conditions. Temporal characteristics of the resulting electron beam showed fast rise times of 3-5 nano seconds (ns) for space charge limited and 8-12ns (full width half maximum) for emission limited cases. Spatial characteristics of the output pulse shape revealed a classic clipped peak amplitude in the space charge pulse but identical characteristics in the emission limited pulse output. Both types of emission produced large current densities up to 91 amps/cm^2. Varying the cathode metal used for the photocathode indicates Zinc (Zn) produced the largest current density, and therefore, the highest quantum efficiency in both space charge and emission limited cases.

20 DISTRIBUTION/AVAILABILITY OF ABSTRACT	21 ABSTRACT SECURITY CLASSIFICATION
☒ UNCLASSIFIED/UNLIMITED ☐ SAME AS RPT ☐ DTIC USERS	UNCLASSIFIED
22a NAME OF RESPONSIBLE INDIVIDUAL Prof. F. R. Buskirk	22b TELEPHONE (Include Area Code) / 22c OFFICE SYMBOL 61Bs

DD FORM 1473, 84 MAR 83 APR edition may be used until exhausted
All other editions are obsolete

SECURITY CLASSIFICATION OF THIS PAGE

Approved for public release; distribution is unlimited.

Photocurrent Generation From Basic Metals, Utilizing a Short Pulsed ArF Excimer Laser

by

Thomas Jay Ringler
Lieutenant Commander, United States Navy
B.S., North Carolina State University, 1974

Submitted in partial fulfillment of the
requirements for the degree of

MASTER OF SCIENCE IN PHYSICS

from the

NAVAL POSTGRADUATE SCHOOL
September 1987

ABSTRACT

An excimer laser used to produce "cold" photoelectrons from common metal surfaces offers an improvement over a standard heated (thermionic) cathode electron source. Photoelectrons accelerated across an anode cathode gap were observed under both space charge limited and emission limited conditions. Temporal characteristics of the resulting electron beam showed fast rise times of 3-5 nano seconds (ns) for space charge limited and 8-12ns (full width half maximum) for emission limited cases. Spatial characteristics of the output pulse shape revealed a classic clipped peak amplitude in the space charge pulse but identical characteristics in the emission limited pulse output. Both types of emission produced large current densities up to 91 amps/cm^2. Varying the cathode metal used for the photocathode indicates Zinc (Zn) produced the largest current density, and therefore, the highest quantum efficiency in both space charge and emission limited cases.

TABLE OF CONTENTS

LIST OF FIGURES

ACKNOWLEDGEMENT

With great appreciation to Dr. D. C. Moir and Dr. S. W. Downey of the Los Alamos National Laboratory, for their guidance, patience and long hours assisting with the Poloroid pictures.

To my wife Leslie for the many hours assisting on the computer.

I. INTRODUCTION

Modern devices, such as accelerators and free electron lasers, require enormous numbers of electrons for their high current electron beams. The quality of the electron source is important when used for injection into an accelerator. Sources used to produce electrons currently consist of three general types. These are thermionic emitters, field emitters and photoelectron emitters, each of which offers different spatial and temporal characteristics. In addition to the general types of emitters, materials used to construct cathodes may further increase the quantum efficiency and enhance desirable characteristics of the electron source.

From the initial observations of Rudolph Hertz in 1887 (where increased current flow was observed across a spark gap exposed to incident ultraviolet light), through Albert Einstein's formulation of the photoelectric equation in 1905, and up through our present day use of excimer lasers, we have continued to make significant improvements in our knowledge of the photoelectric effect. Utilizing Max Plank's energy quantization concept allowed Einstein to explain the photoelectric effect which, prior to that time, could not be explained with electromagnetic theory. Photoelectric research in the 1930's and the 1940's was generally accomplished with electromagnetic wavelengths in the range of 4000 to 7600 Angstroms (Å), corresponding to the region of visible light from extreme ultraviolet (UV) to the far infrared. Wavelengths in the lower ranges of 1900 Å to 2480 Å have only been fully

investigated fairly recently. Both synchotron radiation made available in the 1960's and development of the excimer laser, which can produce consistent high intensity, monochromatic light in the ultraviolet region have permitted further research in this region of shorter wavelengths. Recent advances in pulsed excimer lasers make it possible to achieve high photon fluxes of about 10^{16} photons per square centimeter per second (photons/cm^2·sec), for unfocused beams in the UV region. These recent advances have sparked renewed interest in photoelectron generation using common metals, even though metals in general produce very low quantum efficiencies.

This thesis investigates the relative quantum efficiencies of nine common metals for the production of photoelectrons. An Argon Florine (ArF), excimer laser is used as the illuminating photon source. The results are to be used in determining the best cathode material for construction of an improved electron injection source for the Pulsed High-Energy Radiographic Machine Emitting X-Rays (PHERMEX) accelerator currently in use at the Los Alamos National Laboratory.

II. BACKGROUND AND NATURE OF THE PROBLEM

A. ELECTRON SOURCES

The method used to generate electrons is of significant importance because it influences the electron energy distribution, radial velocity components and momentum distribution properties of the resulting electron beam. These properties are important when the electron beam is used as an injector for an electron accelerator. There are three basic types of phenomena that permit electrons to escape from metal cathodes. These include thermionic, field emission (from large applied electric fields) and the photoelectric effect. The most important of these electron sources are thermionic (heated cathode emission) and photoelectric (photon excitation of the cold cathode atomic electron structure). These major sources have intrinsic advantages and disadvantages which are discussed below.

1. Heated Cathodes

The most utilized electron source is the heated filament, where electrons are "boiled" off the surface of a cathode material. This has the single advantage of producing a continuous electron source of large numbers. However, since the electrons are emitted through thermal excitation of the material, the cathode must be maintained at a very high temperature. High temperatures associated with filaments usually accelerate unwanted chemical reactions. Metals with low melting points are not desirable since they cannot be heated to an efficient electron emission point prior to melting. Usually low melting points are

associated with metals that have lower surface work functions. Furthermore, electrons emitted from thermionic cathodes demonstrate a large spectrum of kinetic energies, and more importantly, show a wide variance in the radial components of momentum that are not parallel to the direction of beam propagation. This means the electrons tend to spread out in all directions as they are emitted. Efficient utilization of this type of electron beam may be constrained unless further beam enhancement methods such as focusing or aperture restrictions are incorporated to remove the undesired divergence effects of the electron beam.

2. Field Emission Cathodes

This process utilizes intense electric fields with threshold strengths on the order of 1.0×10^6 to 5.0×10^7 Volts/Meter (V/M) [Ref. 1] to extract electrons, normally from a tungsten cathode surface. The cathode material is usually unheated, but can also be heated to further reduce the surface work function. In general, the intense electric fields shift the surface potential energy barrier to a lower level where valence electrons in the bulk metal have enough internal energy to tunnel out and escape. An electron beam produced by this method has a large radial momentum component associated with the emitted electrons and usually needs to be focused or restricted by a series of apertures to remove the divergence effects. Use of a restrictive series of apertures may result in a several fold reduction in the beam intensity. This system is inefficient, requiring large amounts of energy to generate the electric fields needed for electron extraction and is complicated to construct as compared to thermionic emitters.

3. Cold Photocathodes

Utilization of the photoelectric effect and application of a workable theory, provides for electron production through photon irradiation of simple metal targets. Although early research was accomplished with continuous light sources, excimer laser technology allows pulsed photon illumination. The production of electrons by this method offers the distinct advantage of not requiring continuous high power as in both the thermionic and field emitter. Incident photons interact with the electron structure of the target, allowing electrons to escape the cathode surface, producing a "cold" electron source. The pulse length of the emitted electrons is directly proportional to the length of the incident laser pulse. The intensity of the incident photon radiation can be used to limited extent for control of electron numbers. The maximum kinetic energy of emitted electrons is a function of the incident photon energy. Electrons escape with maximum excess kinetic energy that is the difference between the incident photon energy and the cathode material's work function and is usually on the order of a few electron volts. Because of energy loss within the material due to electron-electron scattering, there is an energy distribution associated with the emitted electrons. Photoelectrons have relatively small transverse momentum components, and therefore, do not cause a rapid divergence of the electron beam. The disadvantage of this electron source, when using metal cathodes, is that quantum efficiency is very low. Quantum efficiency is defined as the ratio of the number of photoelectrons produced to the incident number of photons. For metals, with incident photon energies below 10 e.v., there is general agreement

that quantum efficiencies will not exceed 10^{-2} [Ref. 2]. Metal quantum efficiencies are usually in the 10^{-4} region. At low incident photon energies (6.4 e.v.), quantum efficiency is calculated assuming one incident photon will generate only one photoelectron, and therefore, its value will not exceed unity. At higher incident photon energies, where secondary electron production may occur within the metal, quantum efficiencies higher than unity may be obtained.

4. Elaborate Cathodes

In addition to simple metal cathodes there are a number of much more elaborate cathodes [Refs. 2, 3] that have been constructed over the last 10 years using exotic combinations of several elements. These usually entail the use of an active alkali metal layer on top of, or combined with, one or two other metals. These cathodes provide very high quantum efficiencies and have good emitted electron momentum characteristics. Current densities up to 200 amps/cm^2 [Ref. 4] with quantum efficiencies as high as 0.2 to 0.3 have been achieved. This is one order of magnitude better than can be achieved by simple metal cathodes. However, these systems pay a price in their complexity. They generally require surgically clean cathode surfaces and suffer intense degradation due to surface "poisoning" from vacuum chamber contaminants. Ultra-high vacuums, on the order of 10^{-10} torr must be maintained. The additional effort required to maintain these systems is an extreme disadvantage.

Of course, there are hybrid combinations of these three types of emitters that may provide improved efficiencies. The addition of thermionic heating in conjunction with field emission or photoelectron

activation can produce more electrons and higher quantum efficiencies, however, it may also degrade the cathode causing untimely replacement.

B. SPATIAL CHARACTERISTICS

A distinct advantage of laser induced photocurrent generation is that the electron beam can be pulsed and that the pulse shape of the emitted electrons can be controlled. The input laser pulse, along with the two distinct output pulse shapes observed in this experiment are shown in Fig. 1. The input pulse is generally Gaussian in shape when the laser gas had been "broken in" and is the case for most of the data acquisition. Output pulses consist of the Gaussian shaped photocurrent

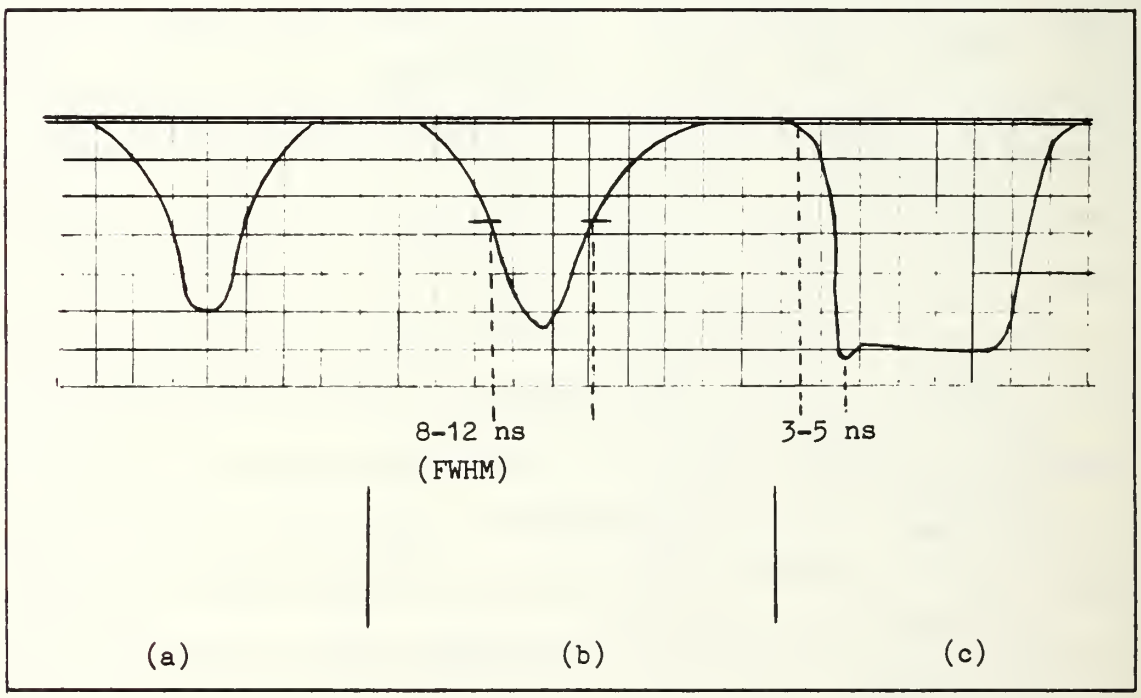

Figure 1. Typical Pulse Shapes of: (a) Laser Output; (b) Photocurrent Output for Emission Limited Flow; (c) Photocurrent Output for Space Charge Limited Flow. Horizontal Scale Shows a Time Base of 5 ns/div, with the Vertical Scale Representing a Variable Output Voltage.

pulse associated with emission limited flow and the "clipped" photocurrent pulse shape associated with space charge limited flow. When emission limited, photoelectrons do not interfere to any great extent with each other as they are emitted. The pulse shape is controlled by the shape of the input laser pulse. Space charge on the other hand, means electron production is great enough to cause those electrons already emitted to interfere with those that are being emitted. The pulse shape in space charge is clipped when electrons outside the metal surface build to a level where they prevent other electrons from emerging. Electron bunches can be generated in repeatable fashion with either of these specific pulse shapes by increasing or decreasing the laser beam power output. For low laser power conditions, a Gaussian shaped output can be obtained. At relatively large power outputs, where the cathode is driven into a space charge limit, a clipped pulse shape is observed.

C. TEMPORAL CHARACTERISTICS

The major advantage of laser produced electrons is the near "instantaneous" production of electrons from photon irradiation of a photocathode material. Following photon incidence, electrons are raised to excited levels within the metal after sub-pico second time delays. This allows direct control of the output pulse length by changing the length of the laser input pulse. It also allows high pulse repetition rates to be achieved when excimer laser pulse technology achieves laser repetition rates in the kilo Hertz region. Pulses observed in this research showed rise times of 8-12 nano seconds (ns) when operating in

the emission limited region. Faster rise times of 3-5 ns were typical when operating in the space charge region. The latter rise time is measured to the point where the space charge limit is reached as shown in Fig. 1.

D. VACUUM REQUIREMENTS

Another major restriction for present photoelectron sources is the requirement for a moderately high to ultra-high vacuum, defined in the range of 10^{-8} to 10^{-10} torr. Although current technology allows ultra-high vacuums to be achieved, simple maintenance and extraordinary efforts are required to sustain the high performance. Ultra-high vacuum systems generally require cathode preparation in "situ" to establish a pure surface and may have to be repeated at frequent intervals to remain at peak efficiency. Great sophistication is required to maintain an elaborate compound alkali metal surface free from mono-layer absorption of gases and other materials which make up the vacuum chamber structure when vacuums of 10^{-10} torr are maintained.

This investigation was performed with only moderate vacuums of 5×10^{-5} to 2×10^{-7} torr. This level was readily obtained within 10 minutes using a Cryogenics, Cryo-Torr-8 vacuum pump.

III. EXPERIMENTAL PROCEDURE

The experiment was designed with simplicity in mind so that further research or a larger scale-up of the photocathode assembly could maintain the same simplicity in construction, reliability, cathode material availability and remain within low monetary constraints. The experimental apparatus for the generation of photoelectrons is shown in Fig. 2.

A. LASER/OPTICAL DESCRIPTION

The excimer laser used as a photon source was an "off the shelf" LAMBDA-PHYSIK EMG-150T. This gas filled laser can be used with either Argon Florine (ArF) or Krypton Florine (KrF) gas to produce an emitted laser beam in the ultraviolet end of the spectrum. Specifically, it can be tuned to either 193.4 nanometers (nm) or 248.0 nm wavelengths respectively. For this experiment, the laser was used in the ArF mode, producing photons with an energy of 6.4 electron volts (e.v.) per photon. The laser was pulsed at 2-3 Hertz (Hz) while determining data, but was capable of repetition rates of several tens of Hz. The laser was mounted, along with most other equipment, on a large optical table. The vacuum chamber, with a volume of about 10 liters, contained the target cathode and collector assembly. It was mounted separately on the floor at the end of the optical table to allow a Cryogenic, Cryo-Torr-8 vacuum pump to be attached as an integral part of the target chamber.

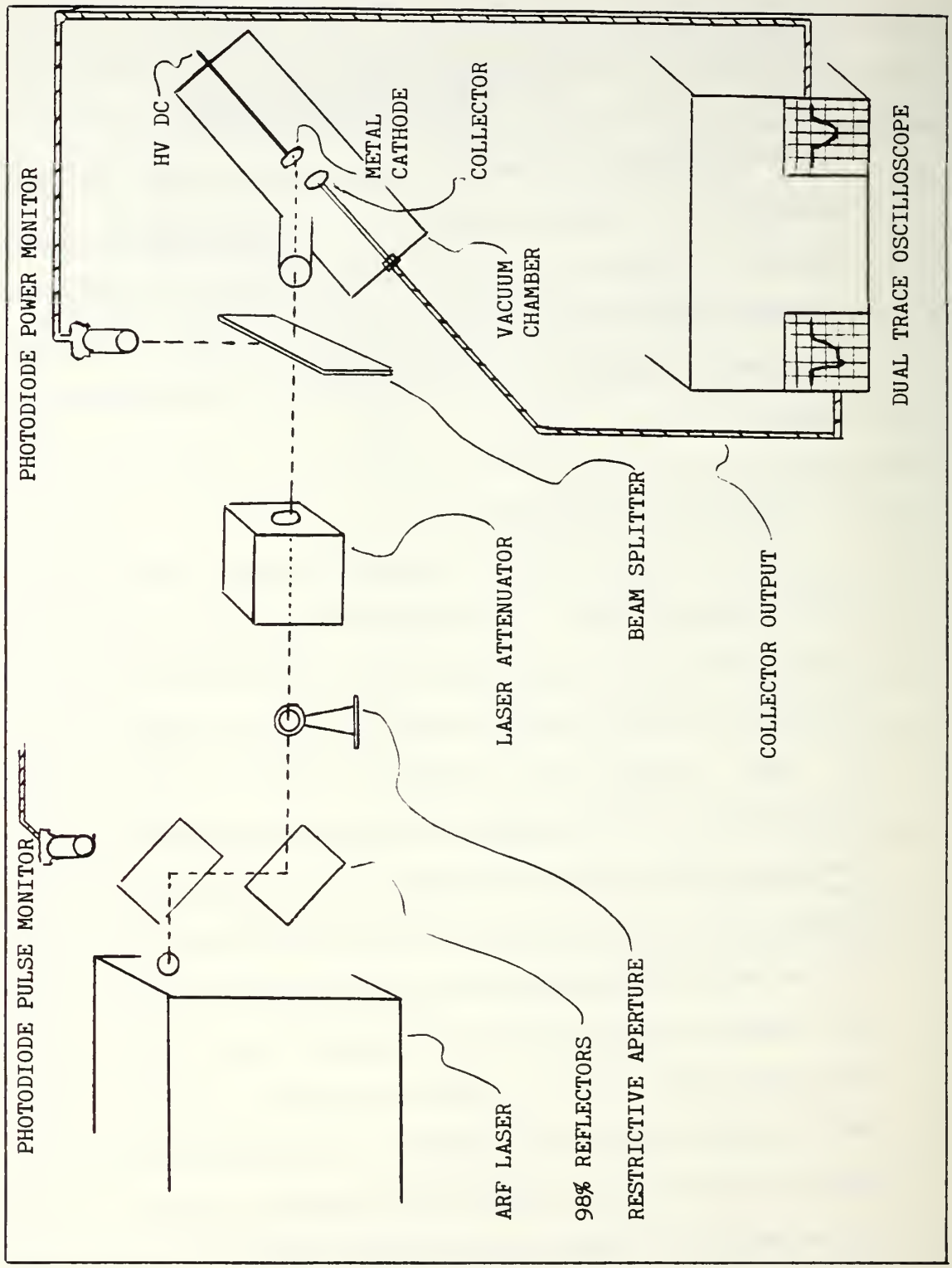

Figure 2. Overall Schematic of Excimer Photocathode Experiment.

As the laser beam exited the excimer laser case it was translated 18 inches lower than the exit height, via two quartz plates adjusted at 45 degrees to the beam path to create a parallel beam path. The quartz plates were 98% reflective for the tuned laser wavelength of 193.4 nm. Translating the path allowed final beam alignment into the vacuum chamber and onto the cathode surface. Additional fine adjustments of the target chamber position permitted the photon beam to traverse internal apertures within the vacuum chamber. One drawback of the photon beam produced by the excimer was the non-circular and the non-homogeneous intensity composition over the beam's roughly elliptical cross section. To obtain a more uniform beam, an adjustable circular aperture was positioned just after the 45 degree reflecting plates and prior to the laser attenuator to allow selection of a circular portion of the beam with fairly uniform intensity characteristics. This also narrowed the beam, allowing it to pass through a NRC Model 935-16 Laser Variable Attenuator, reducing internal scattering and unwanted reflections. A variable attenuator was used to obtain data in the emission limited electron production region. For most emission limited data, intensity reductions on the order of 100 in laser beam power were required. The beam was then passed through a 50% reflecting quartz plate to produce a split beam. One portion was passed to an EGG FND-100Q Ultra Fast silicon photodiode used to monitor the laser pulse shape while the other portion of the beam was passed through a Suprasil entrance window and into the vacuum chamber. The Suprasil quartz window creates the standard 8% loss in transmission due to reflection. A second silicon photocell was used to monitor (from laser beam

scattering) the pulse shape of the laser beam at the first 98% reflecting plate. Beam monitoring was necessary to provide a means of future correlation between individual laser pulse power and the resulting current pulse produced from the extracted photoelectrons at the collecting apparatus. Redundant photocell monitoring was used with the laser in the ArF configuration, to track pulse to pulse instability in the excimer output and also as a master trigger control for the monitoring oscilloscopes.

B. VACUUM CHAMBER AND TARGET CATHODE DESCRIPTION

Two separate geometries were used for photoelectron collection and the cathode arrangement in the target chamber. The first geometry is described below and is shown in Fig. 3. After alignment difficulties appeared and concern arose over the reliability of current collection, geometry improvements for more accurate current collection were effected and are diagramed in Appendix C. Two major improvements to the geometry were increasing the collector area and optimizing the distance from the anode face to the collector surface such that it was 2.5 times the anode aperture diameter. This minimizes any focusing or divergence of the electron beam as it transits the distance between anode face and collector surface.

Upon entering the vacuum chamber, the laser beam was restricted by a circular aperture to project a spot size of 0.0742 cm^2 at the center of a 2.54 cm diameter cathode disk surface. A high voltage direct current (HVDC) potential was maintained across the anode-cathode gap. The vacuum chamber, anode and all other parts of the support structure were

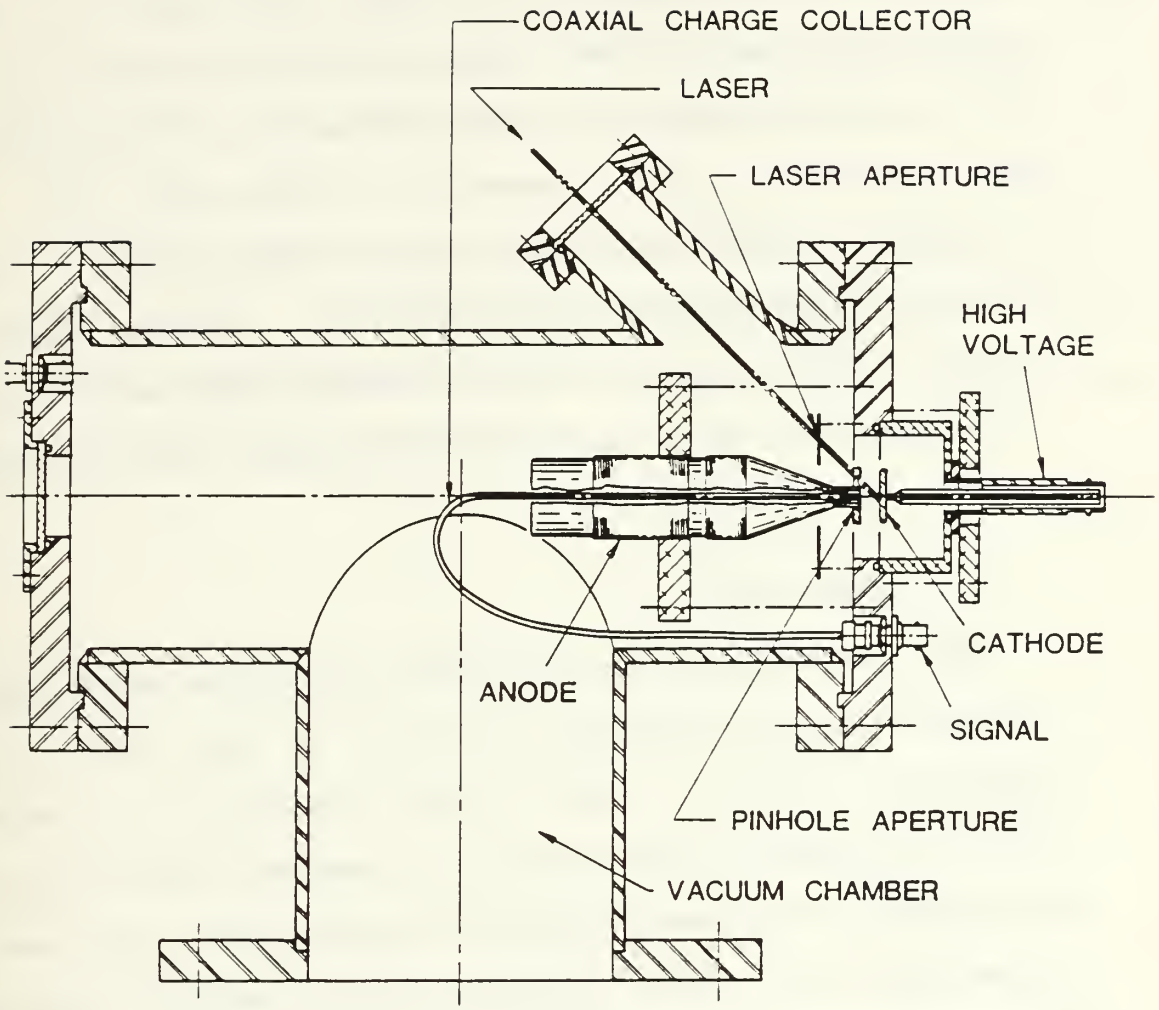

Figure 3. Initial Experiment Vacuum Chamber and Cathode Target.

maintained at ground potential. In most cases, voltages were adjustable up to 29 kilo-Volts (KV) before high voltage arcing occurred in the cable material. Photoelectrons escaping the metal photocathode were accelerated across a 0.332 cm gap towards the anode and the collection apparatus. This photoelectron beam was then restricted by a second aperture of size 0.003167 cm^2, which was an integral part of the anode face, to reduce the final cross sectional area of the electron beam prior to arrival at the surface of the collector cable. The photoelectron beam was collected on the center conductor of a standard coaxial cable with an impedance of 50 Ohms (Ω). Photocurrent generated at the collector was routed from the vacuum chamber and measured as a voltage pulse on a Techtronics R7103 oscilloscope with a one giga-Hertz response capability.

C. DATA ACQUISITION

Experimental data for the nine metals utilized the improved geometry of Appendix C, and were obtained by using the gold cathode as the calibration reference. With the gold cathode set up in the vacuum chamber, the laser was pulsed and the photocurrent (output) pulse shape was monitored. Using an accelerating potential of 4KV, laser power was reduced with the variable attenuator until an emission limited output pulse was obtained. This should have insured an emission limit at all higher accelerating potentials but experimentally this did not occur. Voltage was then increased to 5KV where a set of 16 photos was taken concurrently of both the laser pulse and the photocurrent output pulse. Data sets were repeated at 10KV and 20KV. The cathode metal was then

substituted with another and data sets repeated at 5KV, 10KV, and 20KV. When some of the higher efficiency cathodes were used, they showed only space charge limited flow at 5KV. For these cathode materials, data points were also taken at 15KV. Photos were needed to "freeze" pulses for later analysis. Pulses on the photos were subjectively evaluated for pulse shape (to determine emission or space charge limit). Measurements were made of the peak amplitude, amplitude at full width half maximum (FWHM), time base for the input laser pulse and the photocurrent output, and time base at the FWHM point for the input and output pulses. This information was then manipulated by a computer program written to reduce the data, and determine current density, power per pulse and quantum efficiencies.

IV. THEORETICAL CONSIDERATIONS

A. GENERAL

It is not the intent of this section to offer an all encompasing explanation of the photoelectric process, nor is it intended to quantitatively verify prior models or provide a new model to replace those currently in use. The number of variables required for a total theoretical development is simply too large and an all inclusive theory has not yet been developed. What follows is a review of some basic concepts and a few specific factors that were considered during the conduct of this research. As the entire purpose of this research was to investigate a simple but effective method of electron production, a great many influencing factors are accepted "as is" without an attempt to quantitatively evaluate the degree of influence each provided individually. If an attempt to evaluate and then minimize the adverse effects of all these factors is made, then the simplicity of the research is compromised.

B. BACKGROUND

During the early development of electromagnetic theory, the photoelectric effect was studied as an observed anomoly. With the introduction of quantum theory and the dual wave/particle concept of light consisting of quantum bundles of photons, more complex theories on the interaction of photons with the surface and bulk material of matter emerged. Whether true photoemission is strictly a "surface" effect or

predominately a volume effect has been argued for many years. Where earlier investigations tended to indicate a volume effect, more recent investigations [Ref. 5] and the current trend in relavent information indicates that the surface effect is the main source of photoelectrons. One of the most general and widely accepted theories up through the early 1970's has been the so called "three step" process originally proposed in the 1960's by C. N. Bergland and W. E. Spicer [Refs. 6, 7]. This basic model varies depending on whether the cathode material being considered is a metal or a semiconductor. In general, this section discusses aspects that relate to simple metals unless otherwise specified.

C. THREE-STEP PHOTOEMISSION CONCEPT

The three-step process considers a photon of energy $\hbar\omega$, to interact with, and transfer momentum to, a single electron in the metal. According to basic theories generated in the early 1900's by P. Drude, metals are considered to contain a free flowing "sea of electrons" which exist in thermal equilibrium with the atoms of the metal [Ref. 8]. Incident photons excite this sea of electrons by momentum transfer that imparts enough energy to allow some to escape from the metal.

In step one of the three-step process (Fig. 4a), photon energy is totally transferred to a single electron at a depth (within a metal) ranging up to several hundred angstroms. The penetration depth is usually comparable to the electromagnetic radiation wavelength associated [Ref. 9] with the illuminating photon. Certainly, in metals at the frequencies associated with ultraviolet light, "photons have

depths of penetration...which always are larger than 100 Å" [Ref. 10], with penetration depth being a function of incident photon energy and the material. Photon energy is assumed to be transferred as momentum to only a single electron which then typically responds in a three dimensional collision process. That is, total momentum will consist of the vector sum of the momentum components. Each incident photon interaction transfers momentum that will raise one electron within the metal to an excited level, with energy $\hbar\omega$, above its ground state.

In step two, the excited electron (Fig. 4b), with energy $\hbar\omega$, above the ground state, may undergo no collisions before escaping the metal surface, or it may undergo elastic and inelastic electron-electron collisions until its energy is dissipated throughout the metal bulk or until the collision process results in the electron arriving close enough to the metal surface for it to escape as a photoelectron. For metals, escape depths are generally short. By far, electron-electron collisions represent the greatest energy loss mechanism for excited electrons. The mean free path of the excited (higher energy) electrons in the bulk should be a function of the total electron density (proportional to the atomic number) and the initial energy, $\hbar\omega$, transferred to the individual atomic electrons. Typically, in metals one finds an escape depth of from several angstroms to several tens of angstroms [Ref. 9] depending on the photon energy. Work done using synchrotron radiation in the UV region at the Deutsches Elecktronen Synchrotron (DESY) [Ref. 11] indicates an effective escape depth of about 30 Å for metals. If electrons are excited in the bulk metal below this escape depth, they will not travel far enough in a direction

towards the metal surface to enable them to "escape" as photoelectrons. In addition, even though an excited electron may have enough total energy when it arrives within range of the surface, the critical aspect of its momentum is the component perpendicular to the surface.

In step three of the three-step process (Fig. 4c), if the final perpendicular momentum component is greater than or equal to that required to break through the surface potential barrier (i.e. the work function of the metal) then the excited electron will escape and be emitted as a photoelectron into the adjoining medium (a vacuum for this experiment). This emitted electron may have any kinetic energy (K.E.),

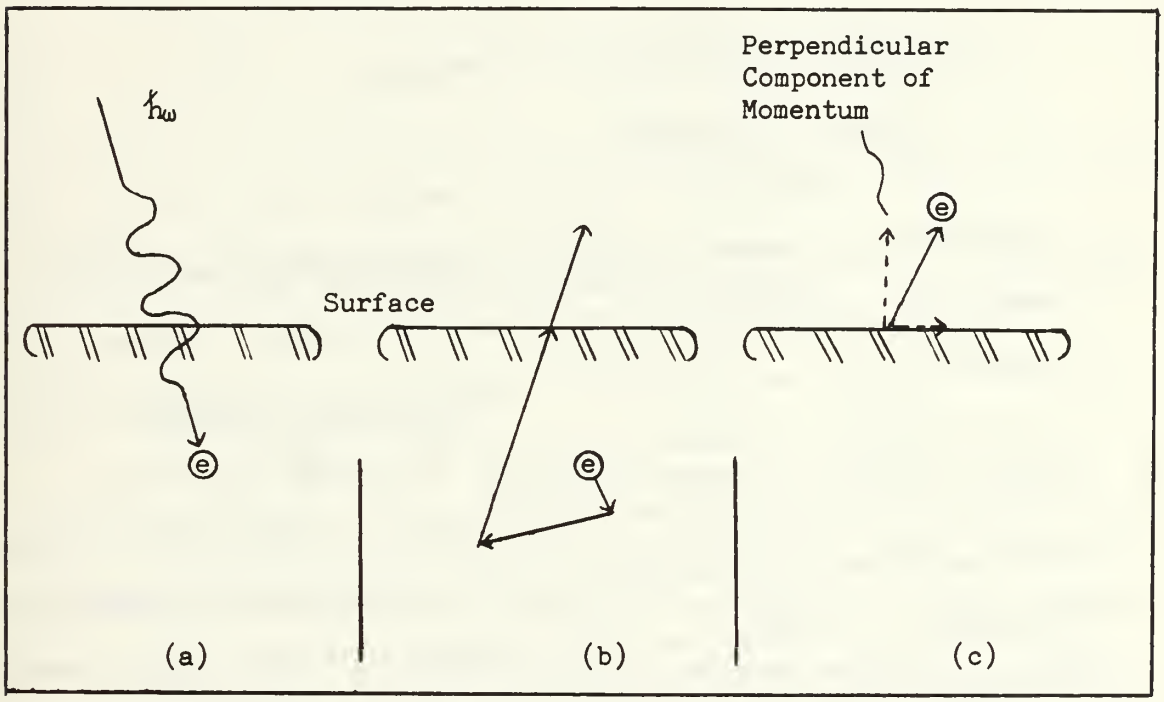

Figure 4. Three-Step Process of Photoelectron Emission: (a) Photon Energy is Totally Absorbed by Single Electron Within Metal; (b) Excited Electron May Undergo Multiple Collisions; (c) Electron Will Escape if Perpendicular Component of Momentum at Surface is Greater Than or Equal to Metal Work Function.

outside the metal surface, up to a maximum energy of $\hbar\omega$, minus the work function (ϕ) of the metal. This last relationship is exactly what Einstein theorized in his photoelectric equation in 1905. That is:

$$K.\ E._{max} = \hbar\omega - \phi \ .$$

The maximum kinetic energy for a photoelectron would correspond to an electron excited at the first atomic layer of the metal surface, which is subsequently ejected with its total momentum component perpendicular to the metal surface. The only energy loss in this case would be due to the work function of the metal.

D. OTHER FACTORS INFLUENCING PHOTOEMISSION

1. Photon Polarization

The simplified three-step process can lead to reasonable interpretations and calculations for photolectron production when either simplified monochromatic or broad band photon sources are used. However, as with any simplified process, other influencing factors need to be considered. Research conducted by J. Barton et al., on angle resolved ejected electron energy curves for copper [Ref. 12], confirms that the polarization direction of the incoming photon energy can have a significant influence on the efficiency of the photon absorption. Generally, higher quantum efficiencies (more photoelectrons produced for each photon) are obtained when the electric field vector for the incoming electromagnetic wave (photon) lies perpendicular to the plane formed by the incoming photon direction and a unit vector normal to the

metal surface as shown in Fig. 5. Although not fully understood, this increased absorption is thought to be due to surface phonon coupling.

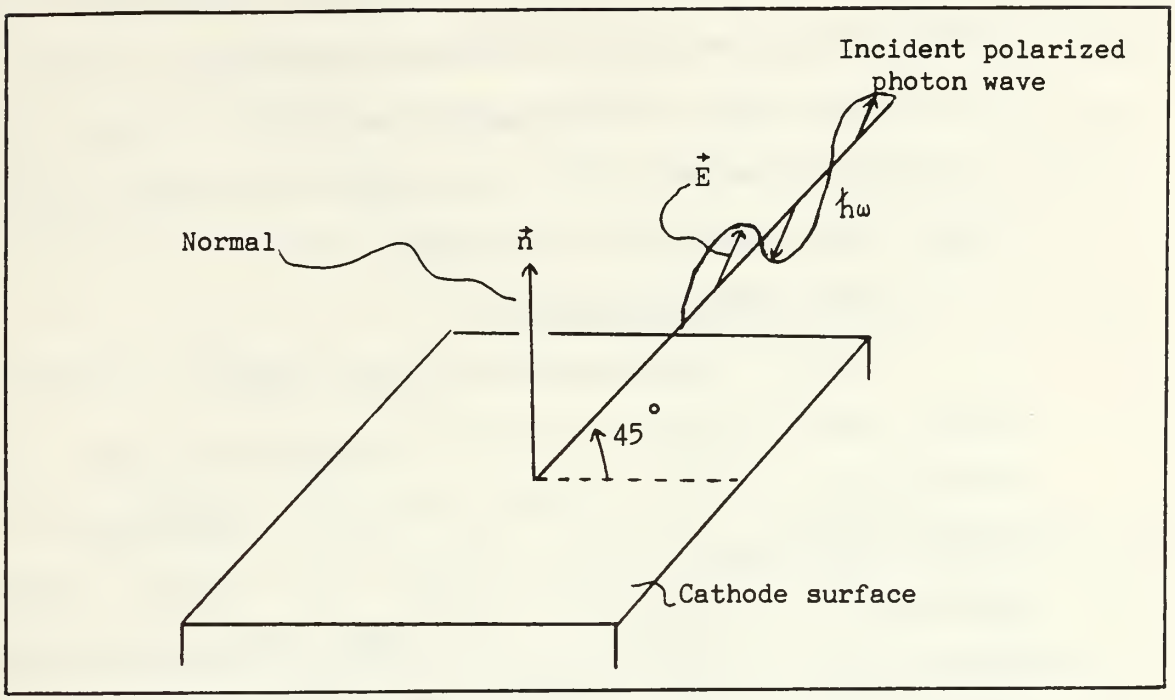

Figure 5. Optimal Geometry for Most Efficient Coupling of Polarized Laser Beam into Metal Cathode Surface.

2. Surface Contamination

In the three-step theory we assume a pure metal surface. In practice, emission is affected by the absorbate layer on the metal surface due to chemisorbtion (chemical interaction with the surface). This chemisorbtion may significantly alter photoemission, by adding or subtracting from the basic work function of the pure metal. This produces a larger or smaller observed work function which in turn will decrease or increase the number of emitted photoelectrons. A monolayer of adsorbed gases will form rapidly in all but the very highest vacuums.

For vacuums of 5×10^{-5} to 2×10^{-7} torr, used in this experiment, expected monolayer formation occurs in 0.1 to 10 seconds on a pure metal cathode [Ref. 2]. If we consider an electron escape depth of 10 Å and a metal lattice constant for the surface contamination of just 4 Å, then the topmost layer of contaminating atoms would contribute about 30% to the photoemission [Ref. 10]. Therefore, the surface layer purity may significantly effect the photoemission.

3. Metal Crystal Orientation

A metal's work function may also depend on the particular crystal plane photons are incident upon [Refs. 2, 13]. For example, expressed as a Miller indexes, the (111) crystalographic plane may produce better photon coupling than the (100) plane. Photoelectron production is a function of the planer densities associated with different crystal planes because of the change in planer atomic electron density. Additionally, the type of crystal structures, such as body-centered cubic or hexagonal-close-packed, also determines how photons transfer their energy to electrons in the metal cathodes.

4. Surface Roughness

Photoelectron production may vary considerably due to surface roughness. This effect is enhanced when large electric fields are applied. The apparent work function may vary as a result of macroscopic features such as larger grain boundaries, dislocation boundaries or microscopic faults in a localized area such as etch pits. Irregularities in the surface structure create intense localized electric fields on the surface protuberances that can initiate field emission or which could cause explosive ionization and plasma formation

above the metal. Additionally, surface roughness will affect the electron beam quality by producing greater divergence of the emitted photoelectrons. It has been proposed that better beam quality (by a factor of five) [Ref. 14] might be obtained by operating a photocathode in the space charge limited region vice the emission limited region. This is due to the greater divergence of emitted electrons from emission limited protuberances, whereas in the space charge limit case, the strong electric fields created by the space charge reduces the radial components of momentum that cause divergence.

E. THE SCHOTTKY EFFECT

The Schottky effect [Refs. 10, 15] is defined as an increase in electron emission (i.e. current) caused by the increasing electric field strength applied between the anode and cathode. Under the influence of an applied electric field, photoelectrons are removed from the area directly above the metal surface immediately. This allows higher photocurrents to be obtained because electrons are not being retarded by the electron cloud which builds up just above the surface. The Schottky effect creates an apparent decrease in the metal cathode surface work function and an apparent increase in the quantum efficiency. The work function is decreased by an amount:

$$\Delta\phi = -C(eE)^{0.5}$$

where E, e and C are respectively the electric field strength in kilo-Volts, the charge on an electron and a constant. This apparent

change in the work function is very small and can usually be neglected unless intense electric fields are used. Generally fields on the order of 5.0×10^7 V/M will decrease the work function by only 0.4 volts. For this experiment the effect was deemed negligible.

F. PLASMA FORMATION

Due to the intensity of the pulsed laser power delivered to the cathode, it might be expected that the metal would be heated locally at the surface, and possibly in the bulk, by inelastic collisions and the creation of surface phonons. A certain amount of thermal activity will occur but its contribution to enhance electron emission via thermionic electron production from the laser "heated" cathode should be minimal. With the laser pulse duration on the order of 30ns, a laser repetition rate of 3 Hz and about 0.016 mj per pulse delivered to the surface, the total power delivered would be about 9.9×10^5 Watts. However, since a portion of the incident energy is reflected, the actual power on the surface would certainly be less by a minimum of 20% for all the metal cathodes.

In general, it is unlikely that 9.9×10^5 Watts would be high enough energy delivery to vaporize and ionize the surface layers on the cathode material. Higher local concentrations may have occured as electric field strengths increased but were assumed negligible. Therefore, plasma formation and the resultant production of secondary electrons created from positive ion bombardment of the cathode surface can be neglected.

V. EXPERIMENTAL RESULTS AND DISCUSSION

The preliminary experiment objective was to determine whether current densities greater than 20-30 amps/cm^2 could be achieved from a laser driven cold photocathode. This value was chosen as a threshold because it is the present capability of the thermionic electron gun in operation at the Los Alamos PHERMEX accelerator. A goal of 50 amps/cm^2 was desired to allow a 100% improvement in the capacity of the present PHERMEX thermionic electron source. In addition, a simple laser driven cold cathode electron source would offer a vast improvement in simplicity and maintenance. Results of the initial investigation in April 1986 [Ref. 16], demonstrated the feasibility of this improvement with experimental current densities of 50-70 amps/cm^2 achieved in emission and space charge limited regions for a copper cathode. Further investigation, and the primary objective of this thesis, was directed towards comparing electron production from several metals to determine which cathode material would produce the highest quantum efficiency.

A. CATHODE MATERIALS AND WORK FUNCTIONS

Nine different metal cathode surfaces were used for this experiment. Eight samples were stock metals that had been diamond machined to a 2.54 cm diameter disk that was 0.40 cm thick. The ninth sample was a copper cathode base that was plated with 1000 Å of gold. In general, metals were of high purities exceeding 99%. After machining, no further attempt was made to highly polish the surface or remove surface

irregularities. Prior to testing, each cathode was "cleaned" for several minutes with lens paper to clear away any obvious surface residues. The cathode surfaces were not microscopically examined prior to testing. Electron microscope examination of the surface of the aluminum and copper cathodes after extensive experimentation, revealed some deep machining marks of about 7 microns in width but otherwise a fairly smooth featureless surface. It was estimated that surface protuberances were no larger than 10 microns. Metals used as photocathodes in this experiment are listed in Table I. They are ordered from highest to lowest in their relative quantum efficiencies (Q.E.) and were evaluated at three anode-cathode accelerating voltage of 10KV, 15KV and 20KV.

It was expected that the relative quantum efficiencies might correspond directly to the relative ordering of the metal work functions which are also listed in Table I. In general, a trend was observed which can be interpreted as indicating that the lower the metal's work function the higher the experimental quantum efficiency. Variations in quantum efficiency and work function ordering can be explained in several ways.

First of all, values for work functions are generally given for "pure" metals, which the experimental cathodes were not. Secondly, the accuracy of any given value for a work function is questionable. When checking multiple references, there is never a single value referenced for an individual metal's work function. Usually a range of values is found, since there are many factors (as delineated in the theoretical considerations section) that influence photoemission and ultimately the

experimental determination of work functions. Accepted values [Ref. 2] listed in Table I, were determined from several techniques, which include both photoemission and thermionic emission. The conditions established for vacuum, temperature, surface contamination, metal purity, metal crystal orientation, surface or bulk emission, ect., all effect the ultimate assignment of a work function value. Therefore, these values are guidelines and should not be used for absolute comparisons unless they are all determined under exactly the same conditions by the same experimental procedure.

Thirdly, the metal work functions spanned only 1.23 volts between the nine metals tested. Most varied only several tenths of a volt between them. It was not possible under the accuracy conditions established in this experiment to determine if work functions had a direct effect on the relative quantum efficiencies.

TABLE I

RELATIVE QUANTUM EFFICIENCY DETERMINATIONS

Q.E. ORDER	CATHODE METAL (10 KV)	WORK FUNCTION (e.v.)	CATHODE METAL (15 KV)*	CATHODE METAL (20 KV)
1	Zinc (Zn)	-- 4.24	Sn	Zn
2	Tin (Sn)	-- 4.50	Zn	Al
3	Aluminum (Al)	-- 4.20	Cu	Cu
4	Copper (Cu)	-- 4.54	Al	Au
5	Gold (Au on Cu)	-- 4.92	Au	Ni
6	Magnesium (Mg)	-- 3.68		Sn
7	Nickel (Ni)	-- 5.01		Mg
8	Stainless Steel(s-s)	-- 4.77		s-s
9	Tungsten (W)	-- 4.69		W

* Incomplete data obtained for comparison, on metals not listed.

B. LASER PULSE/PHOTOCATHODE OUTPUT CORRELATION

Much attention was directed towards perfecting an adequate method to correlate the power of a specific laser pulse and its resulting current density calculated from the photocathode output. Approximately 16 individual laser pulses, monitored at the photodiode (for power correlation) and the collector output, were photographed for each metal cathode. This was repeated at three accelerating potentials. Values obtained from photographs were statistically evaluated by a computer program. Four iterations were performed to smooth the power calculations, with laser pulse power outputs outside two standard deviations eliminated after each iteration. The remaining points were used to calculate the average power, and from that the cathode quantum efficiencies. The relationship between photodiode output (which is proportional to laser power) and the photocurrent densities was expected to be linear for a particular metal at each accelerating voltage. Results obtained for emission limited outputs at 20KV accelerating potential are plotted in Fig. 6, and show the expected linear relationships.

As the anode-cathode accelerating voltage was decreased, it became evident from plotted data that the high quantum efficiency metals were transitioning from emission limited electron flow to space charge limited flow. The distinctive change to a vertical slope (of plotted laser power input to the photocathode surface and the resulting photocurrent output), reaches a maximum value and then remains constant regardless of the input laser power. This is the space charge limit. Here, as anode-cathode accelerating voltage is decreased, maximum

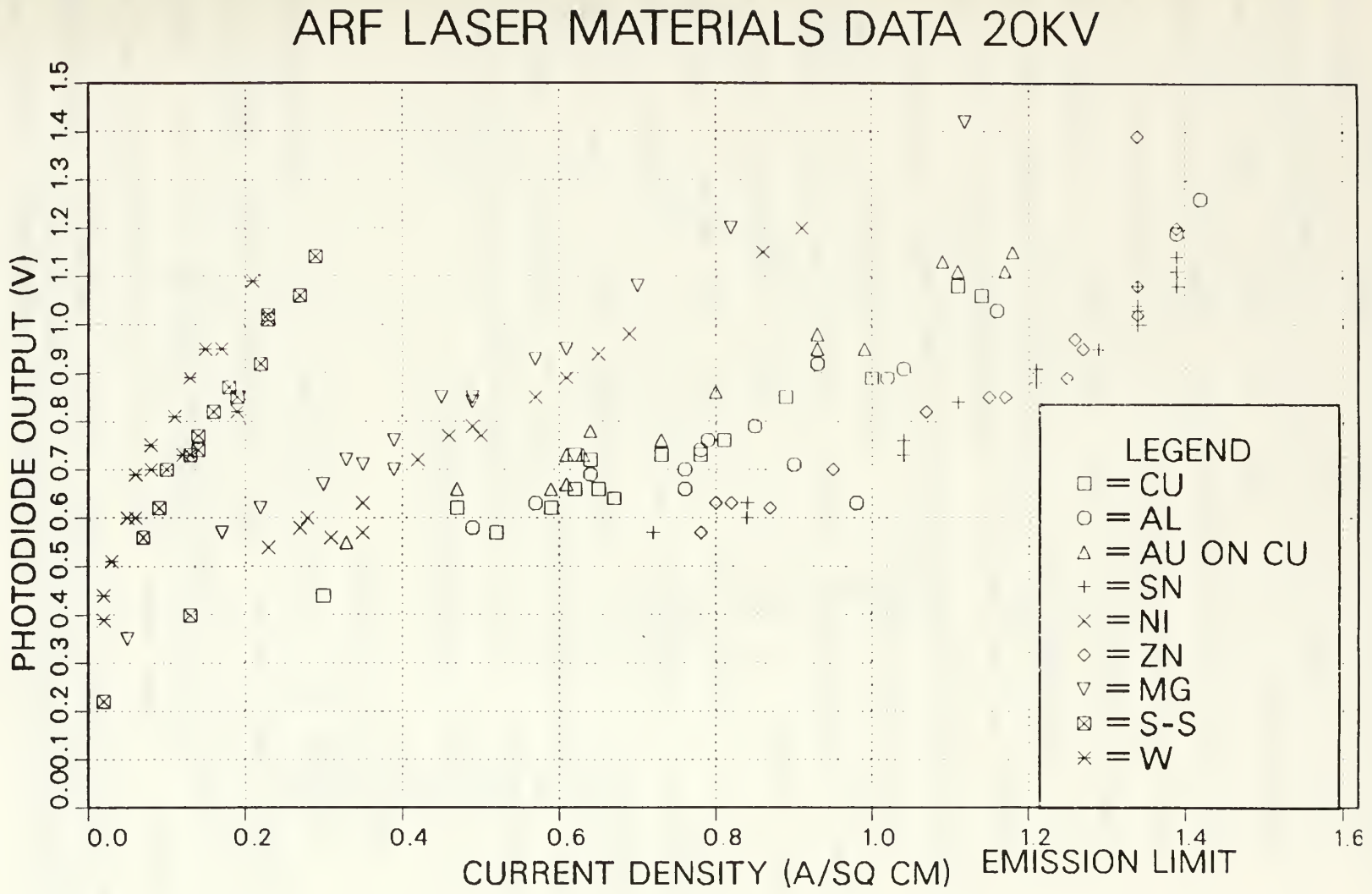

Figure 6. Nine Cathode Materials Plotted at 20KV, Showing Correlation of Photodiode Output to Computed Current Density Generated at the Collector.

electron flow to the collector is prevented due to an intense electron "cloud" build-up outside the surface of the cathode. This condition is evident in the plots of Fig. 7 and Fig. 8, where the slope of the plotted data suddenly becomes vertical. When this limit is reached, no further increase in electron collection can be expected as accelerating voltage is decreased or as the laser intensity is increased. However, if the anode-cathode accelerating potential is increased, the cloud of electrons can be prevented from accumulating since photoelectrons are removed across the gap immediately as they escape the surface.

Although most of the high current density data was obtained in the space charge region, to produce photoelectrons most efficiently one would operate in the emission limited region where electrons do not bunch and interfere with each other after emission from the metal surfaces. In addition, less laser power is required to produce photoelectrons in the emission limited region. It was estimated that this particular LAMBDA-PHYSIK could be attenuated 100 times in power output and still achieve the maximum number of electrons from the metal cathode at 10KV accelerating voltage.

C. CATHODE REFLECTIVITIES

The main goal of this experiment was to determine an "as is" relative ranking for the nine tested metal cathodes. Reflectivity is not a factor in this determination, nor is it of any practical importance unless laser power is of very low order and the goal is to maximize the quantum efficiency. However, the absolute amount of photon energy absorbed by a particular metal cathode will depend on the

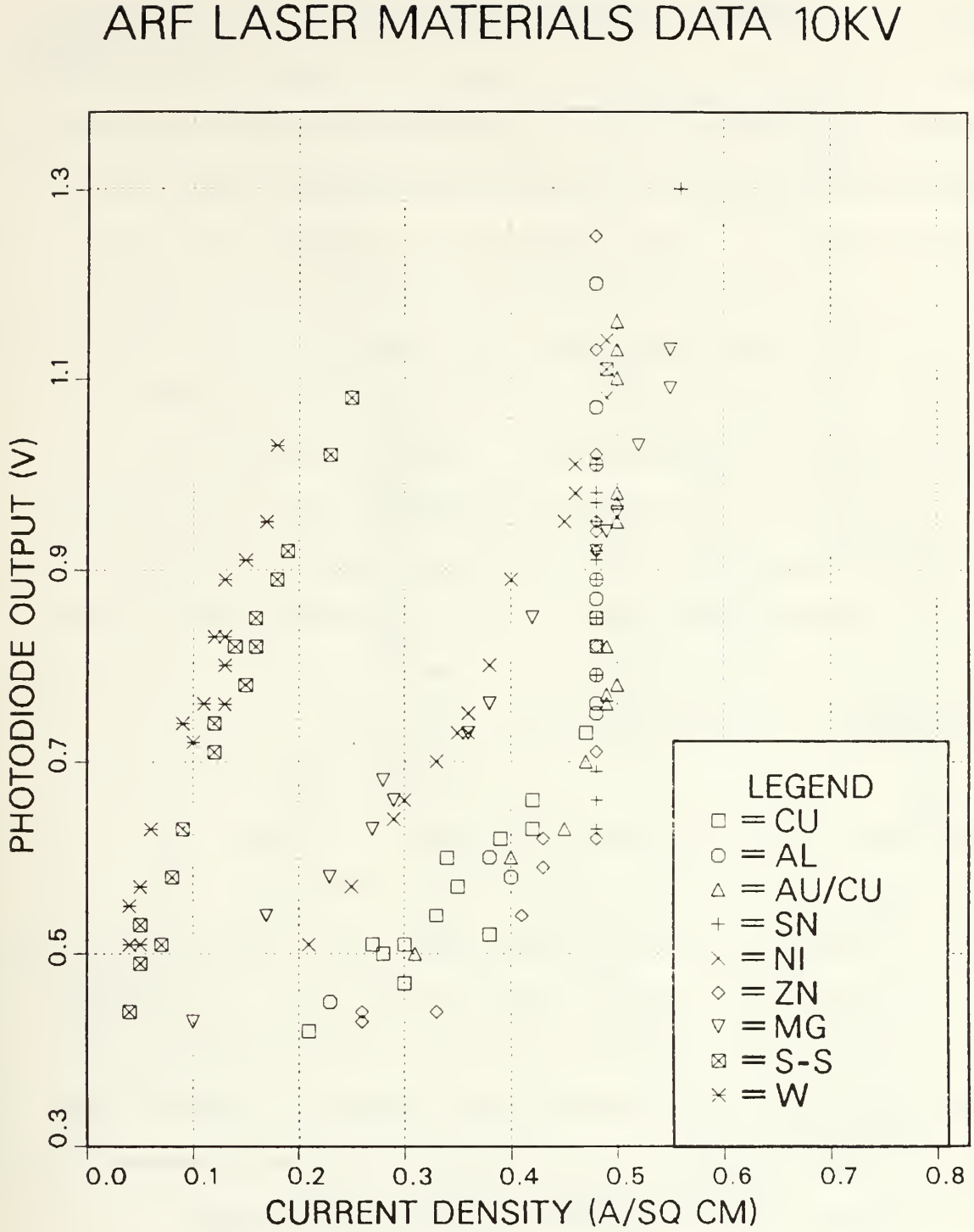

Figure 7. Nine Cathode Materials Plotted at 10KV, Showing a Linear Slope for Emission Limited Flow Changing to a Vertical Slope as Space Charge Limit is Reached.

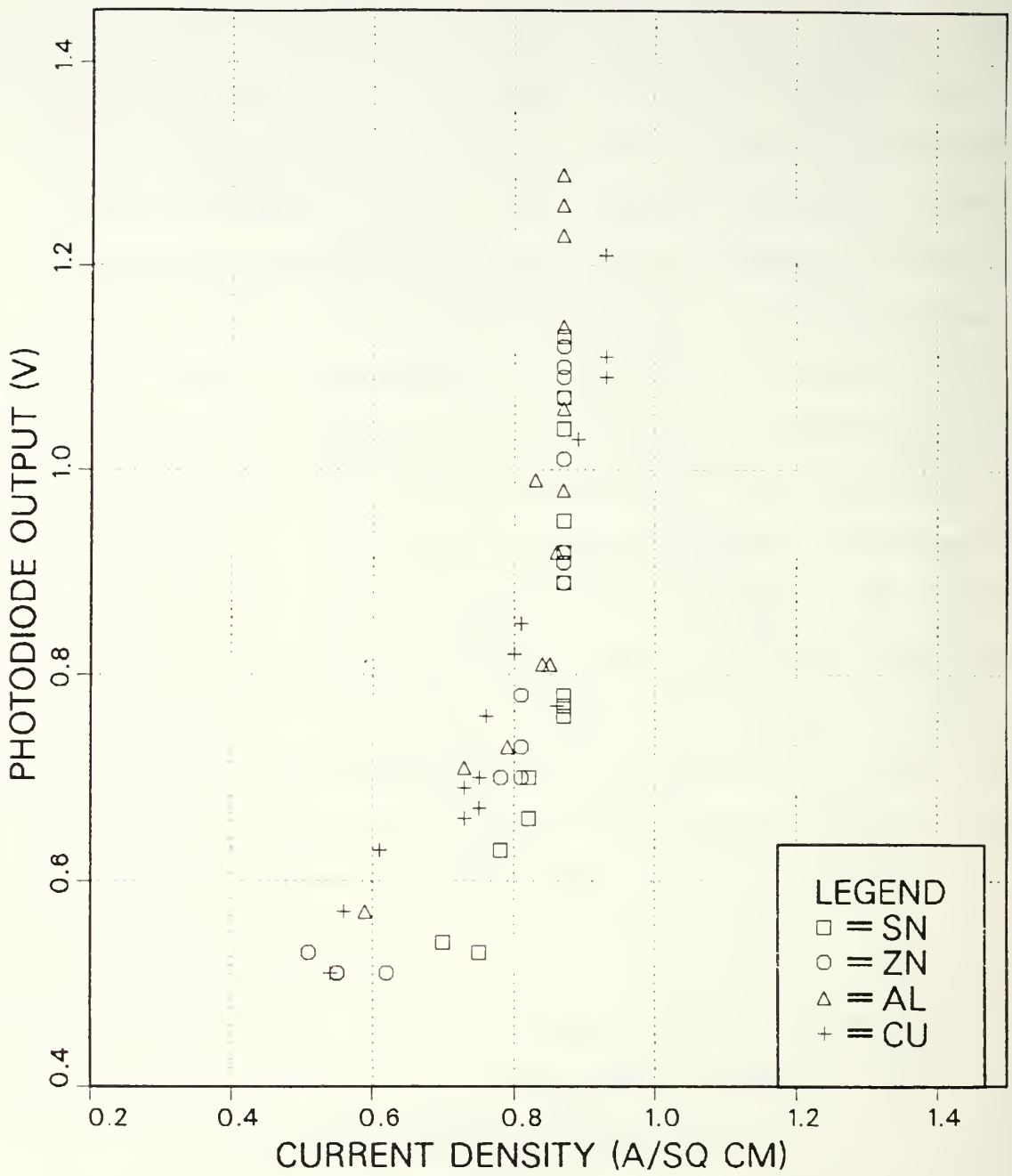

Figure 8. Selected Cathode Materials Plotted at 15KV, Showing a Linear Slope for Emission Limited Flow Changing to a Vertical Slope as Space Charge Limit is Reached.

reflectivity of the surface at the particular incident photon wavelength involved. An attempt was made to determine the absolute quantum efficiencies of the metal cathodes by using experimentally determined reflectivities. Cathode reflectivity was experimentally determined from the ratio of the measured incident energy normal to the cathode surface as compared to the measured energy reflected when the cathode was placed at 45 degrees to the incident path. This energy ratio was accomplished with a Gentec-200 calorimeter and had an accuracy of ±4%. The ArF laser was attenuated so that an average power of 100 KWatts/cm^2 was developed at the cathode surface when determining the reflectivity. The lower laser power was used to minimize pulse to pulse laser fluctuations inherent in this LAMBDA-PHYSIK laser at high power settings and also to reduce the possibility of plasma formation on the surface which could have affected the reflectivity calculations. Values for experimental reflectivity are listed in Table II.

As a quick comparison, theoretical values calculated using known reflectivity relationships and optical constants for the metals [Ref. 17] are also listed. These comparison values assumed a random polarization of the incident laser beam and a laser beam angle of incidence that was normal to the surface. Although this represents a 45 degree difference in incidence angle between the two values, the angular difference is deemed to have a small effect at this photon wavelength. Values not listed are due to lack of available optical parameters for calculations.

The experimental values for reflectivity show that in all but one case (aluminum) the reflectivities vary by just ±6% about an average

value of 26%. Only in the case of aluminum, which indicated a very high reflectivity, would an "absolute" quantum efficiency ordering change its Q.E. ranking in Table II. This deviation is a significant amount and would make aluminum the best metal cathode tested on an absolute scale.

TABLE II

CATHODE REFLECTIVITIES

CATHODE METAL	EXPERIMENTAL REFLECTIVITY (percent)	CALCULATED REFLECTIVITY (percent)
Zinc (Zn)	25	--
Tin (Sn)	27	--
Aluminum (Al)	60	92
Copper (Cu)	25	34
Gold (Au on Cu)	20	21
Magnesium (Mg)	25	--
Nickel (Ni)	32	35
Stainless Steel (s-s)	25	--
Tungsten (W)	27	65

D. LASER POLARIZATION

For this experiment we consider the laser radiation to be a monochromatic plane wave of frequency ν , and energy $\hbar\omega$, incident onto a bulk cathode metal. Because the source of incident radiation was an ArF excimer laser, the incoming wave assumptions are plausible. Normally we might expect the laser photons to be highly polarized due to multiple internal reflections from partial mirrors on the ends of the laser cavity. For this particular LAMBDA-PHYSIK, however, there are few multiple light passes between the laser mirrors prior to the laser pulse discharge. Estimates of beam polarization indicate 80% random

polarization and a 20% horizontal polarization. No attempt was made to fully polarize the laser beam horizontally, or vertically, to assess effects. It is probable that an increase in absolute quantum efficiency could be obtained with a laser beam that is totally horizontally polarized.

E. CHILD-LANGMUIR FLOW

It was observed that electron production as a function of accelerating potential applied to the anode-cathode geometry was consistent with the theoretical Child-Langmuir flow [Ref. 13] calculated for a planer diode arrangement. A predicted space charge limit on current density was calculated using the relationship:

$$J = K \frac{V^{1.5}}{d^2},$$

where J, K, V and d are the current in A/cm^2, perveance in $AV^{-1.5}$, accelerating potential in volts, and anode-cathode separation in centimeters. The assumed planer diode geometry uses a perveance (K) of 2.334×10^{-6} $AV^{-1.5}$ [Ref. 18]. Perveance is identified as a measure of the effectiveness in confining the space charge of the electron beam.

Experimental data for two copper cathode arrangements and the theoretical space charge limit are plotted in Fig. 9. It shows that the experimental output was slightly less in all cases over what is predicted from the space charge limit. This plot is based on the use of a copper cathode with the first experimental geometry but is representative of the response observed for each of the nine cathode metals used with the second geometry.

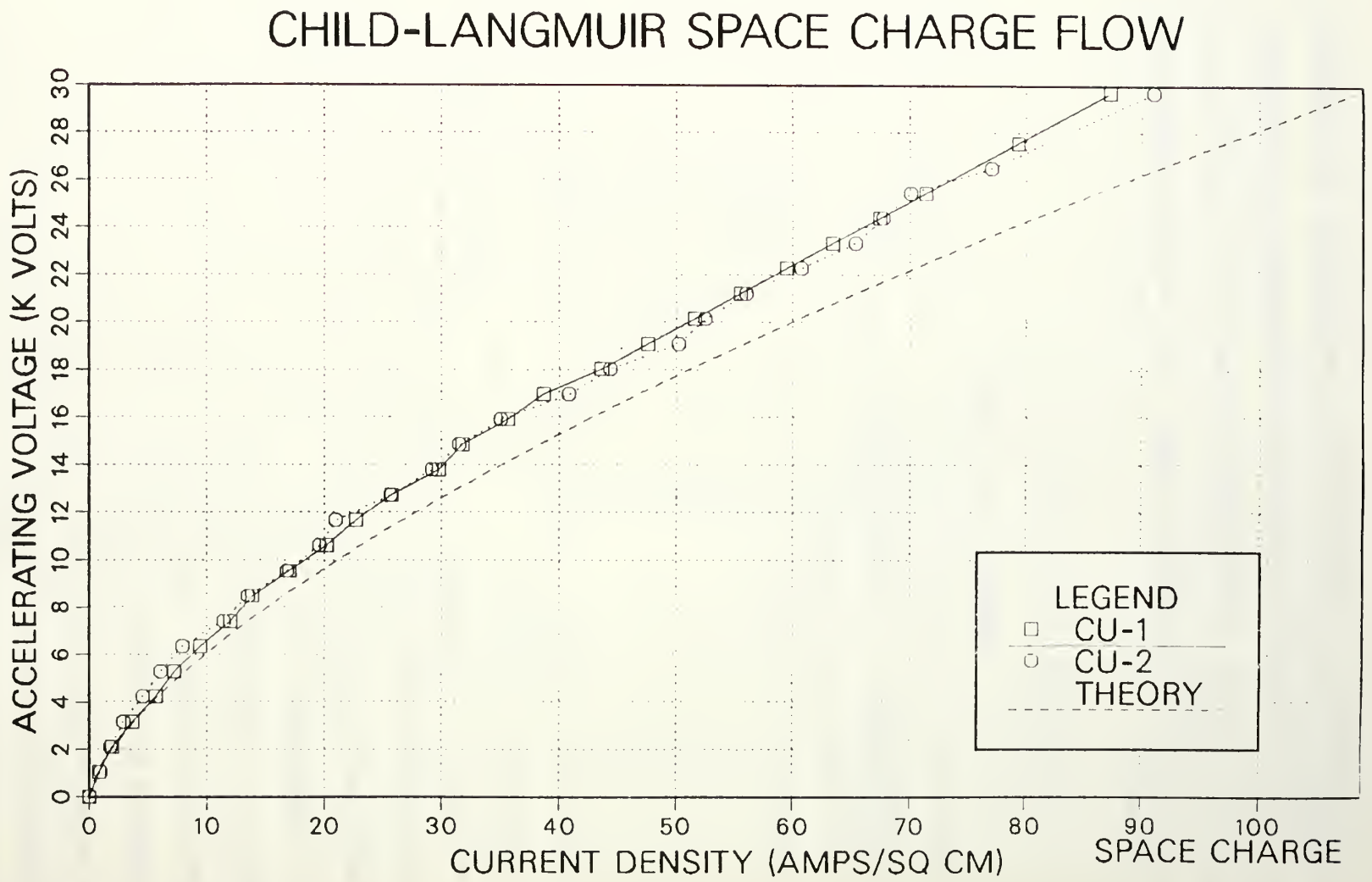

Figure 9. Comparison of Current Density vs Anode-Cathode Accelerating Potential for Theoretical Space Charge Limited Flow and Two Sets of Experimental Space Charge Data.

Additional factors considered that could have produced higher current densities in the experimental setup were ion production and secondary electron production due to electrons impacting the edge of the anode restrictive aperture. These contributions were not individually assessed in this experiment.

The fact that positive metal ions might be increasing current due to secondary electron generation after impact with the cathode surface was considered. However, the observed pulse shapes of the output current did not show any distortion nor any "tails" compared to the input laser pulse shape. The ions being heavier and slower would have added a delayed pulse shape distortion if present. None was observed.

In addition, secondary electrons generated from primary electron collision with the edges of the anode aperture would cause increased current with little alteration in output pulse shape and would have increased the observed difference in the experimental data and the theoretical space charge limit plotted in Fig. 9.

Excellent correlation between theoretical and experimental derived data plotted in Fig. 9, occurs when electron backscattering from photoelectrons impacting the collector surface is considered. The collector surface (center of the coax cable) was made of aluminum. From backscattering data run by a computer program [Ref. 19] at Los Alamos, we know that 20KV electrons impacting aluminum would produce about 15% backscatter. Lower energy, 10KV electrons would produce about 8% backscatter. These backscattered electrons are lost and do not contribute to the output voltage pulse, making the experimentally calculated photocurrent lower than its actual value. If just the

backscattering percentages are incorporated, then the theoretical and the experimental values agree within 2% at 20KV and 7% at 10KV. Known experimental errors were determined to be ±2% due to measurements of the physical geometry and ±2% in measurement of the accelerating potential, producing a maximum error of ±7%.

F. CURRENT DENSITIES ACHIEVED

The experimental electron current density, J, was calculated using the illuminated collector area and the output voltage pulse from the relation:

$$J = Z/R\ (1/\text{Area}),$$

where J, Z, R and Area are the photocurrent density in amps/cm^2, photocathode output in volts, 50Ω impedance of the collector cable and the final illuminated area of the collector surface respectively.

As there were two different geometries used in the experiment, the magnitude of the measured current densities varied. Maximum values of 91 A/cm^2 for both emission and space charge limited data were obtained with the first geometry. This first geometry, with a small anode-cathode gap, produced electric field strengths up to 89 KV/cm. Values of less than 2 A/cm^2 were obtained with the second geometry. These lower values were due to the lower electric field strengths of up to 13 KV/cm, and lower laser power due to required attenuation. The lower electric field strengths were due to a larger separation in the anode-cathode gap. However, because current density is spread over a much larger collector area, the total current is comparable. The

objective with the second geometry was to obtain a relative comparison of quantum efficiency for the metal cathodes and not to maximize current densities.

G. RELATIVE QUANTUM EFFICIENCY DETERMINATIONS

Relative quantum efficiencies are related to the experimental results only when emission limited data is considered. Relative quantum efficiencies experimentally determined at 20KV accelerating voltage are displayed in Fig. 10. Relative quantum efficiencies determined at 15KV accelerating voltage are shown in Fig. 11. These nine metals are further listed in Table I, in order of decreasing Q. E.. In general, the ordering was consistent between metal cathodes at the three accelerating voltages tested. Deviations were thought to be due to the pulse to pulse power changes in the laser which led to inaccurate power determinations. Quantum efficiencies (η) were calculated using the relationship:

$$\eta = 6.41 \frac{J}{P},$$

where J and P are the photoelectron current density in amps/cm^2 and power in Watts/cm^2 respectively. The constant 6.41 is the quantum energy (in electron volts) for a photon with a wavelength of 193.4 nm.

From Fig. 10, we note that the highest and lowest relative Q. E. are separated by about one order of magnitude between the nine cathode samples. The experimental accuracy in determining power allows at best a qualitative validity to these orderings. Comparisons between groups of metals as having a higher Q. E. can be recognized, but an absolute

comparison between individual Q. E. or an absolute scaling of the Q. E. can not be made. It would be fairly accurate to say that zinc demonstrates a better Q. E. than stainless steel but not necessarily correct that aluminum is much better than copper in quantum efficiency.

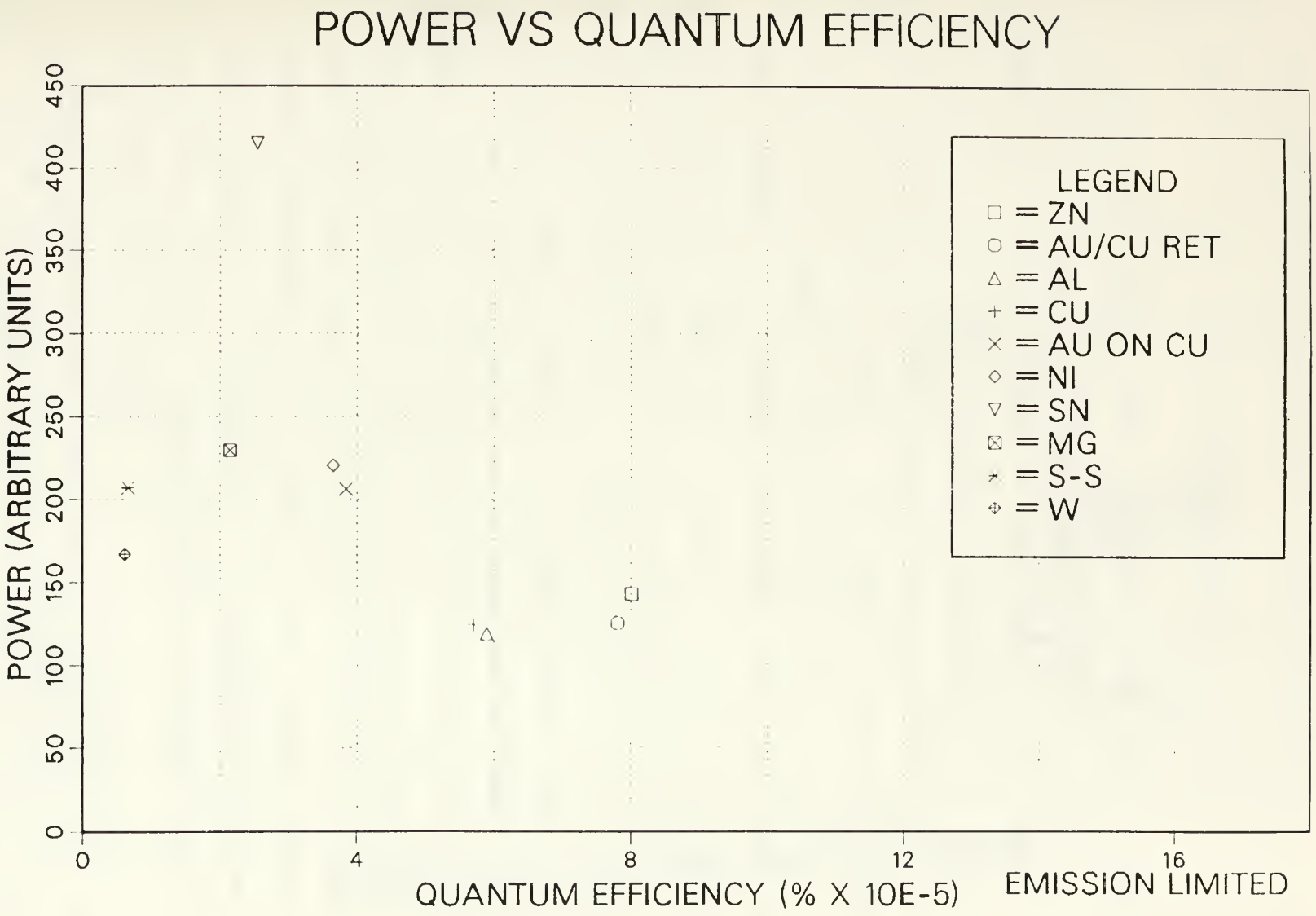

Figure 10. Relative Quantum Efficiency Comparison at 20KV Accelerating Voltage.

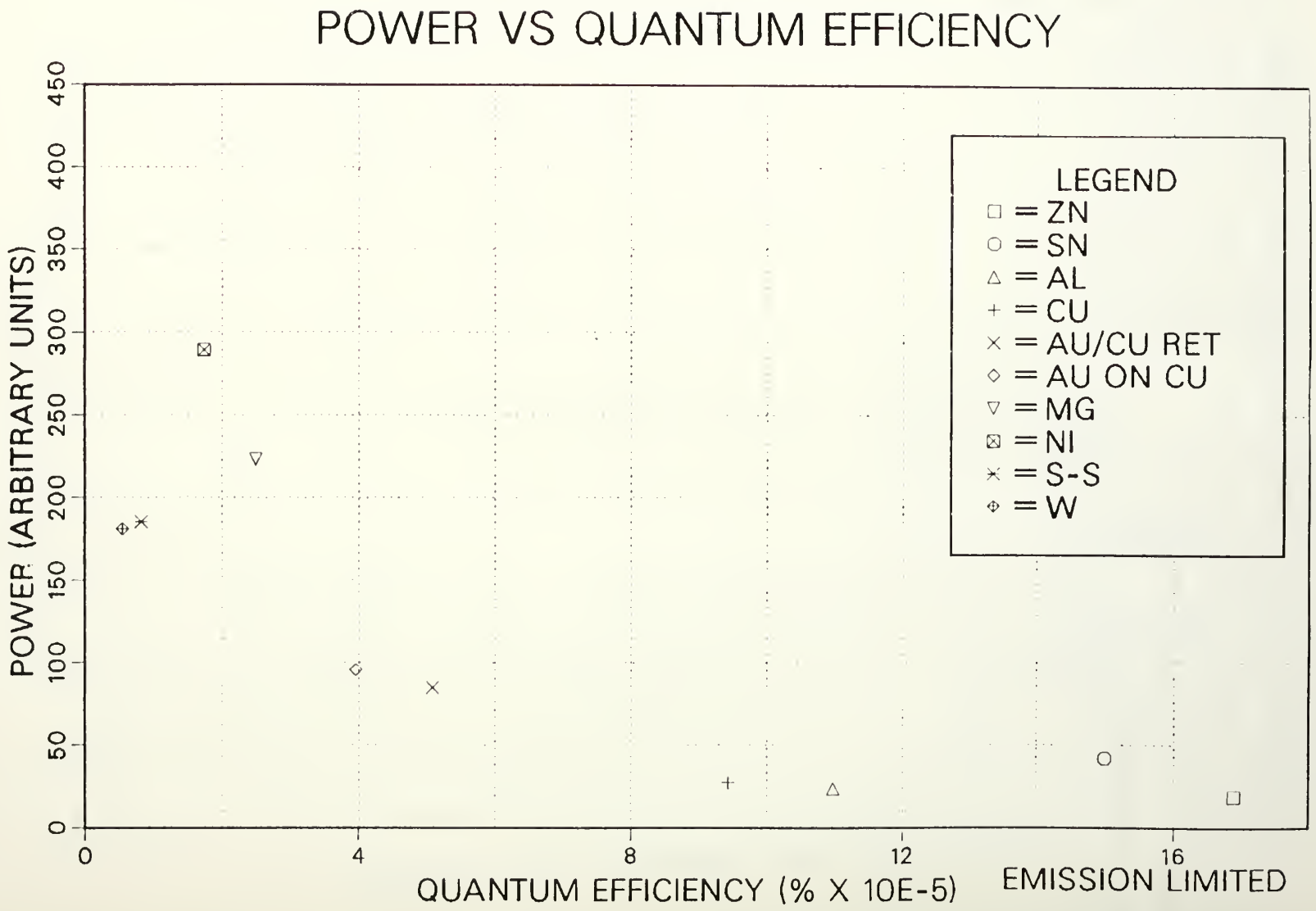

Figure 11. Relative Quantum Efficiency Comparison at 15KV Accelerating Voltage.

VI. CONCLUSIONS

Using an ArF excimer laser to generate "cold" photoelectrons, an experimental investigation was conducted on nine metal cathodes. The primary goal of the experiment was to perform a relative evaluation of the quantum efficiencies (Q.E.) for the metal cathode materials. Results showed, with an anode-cathode accelerating voltage of 20KV, that for the nine metals tested, zinc produced the highest quantum efficiency. Tin, aluminum, copper and gold followed as a group, and ranked higher as photoelectron emitters than nickel, magnesium, stainless steel and tungsten as a group. It must be remembered that these are relative rankings and that the actual quantum efficiencies of metals are generally poor. Attempts to calculate relative quantum efficiencies produced values for the nine metals that range from 2×10^{-4} to 1×10^{-5}. These values are lower than the generally agreed maximum value of 10^{-2} obtainable with 10 e.v. photons and pure metals but do closely approach the general Q.E. value of 10^{-4} for metals. As calibration of the laser pulse power was not very reliable, experimental calculation inaccuracies could account for the apparent disparity in these efficiencies. Furthermore, if reflectivities are taken into account, then Q.E. may be compared favorably to accepted values in the 10^{-2} to 10^{-4} region for metals.

Additional results demonstrated a current density of 91 A/cm^2 could be achieved with a copper cathode at 29KV accelerating potential. Reflectivity determinations indicated that only aluminum had a

substantial reflectance. If an absolute comparison of the nine metals were considered, this would translate to aluminum producing the highest quantum efficiency.

It would appear that, even utilizing simple metals, photoelectron sources can be manufactured that would offer large current densities and tailored pulse shapes. These photocathode sources would also provide the added advantage of being easy to construct and maintain.

Presently, initial results of this research are being utilized to incorporate a practical working electron gun into the PHERMEX accelerator. The first test cathode is being constructed from lead, which was evaluated as a more efficient photoelectron source than zinc, as suggested by a parallel thesis investigation [Ref. 20]. It would appear that even denser metals may present still better quantum efficiencies.

The full theory of photon interaction with metal cathode surfaces is in general not fully understood. Although extensive research continues on individual facets of the overall processes involved in photoelectron production, a complete theory encompasing all the variables associated with the photoelectric effect has not been promulgated.

VII. SUGGESTED FOLLOW UP EXPERIMENTATION

Investigations into the more efficient utilization of the laser pulse could be made. Determining the minimum power requirements for electron production would also be valuable information. This would entail an experimental setup to determine the laser pulse power on an absolute scale.

The two photon excitation concept may be a method to improve the coupling of photon energy delivered to the cathode. Using attenuated total reflection (ATR) [Ref. 21], which uses two cathode plates placed at 90 degrees to each other, an increase in photoelectron quantum efficiency may be possible. However, because this would involve a change in the planer geometry arrangment, it may detrimentally alter the electric fields between anode and cathode and adversely affect the electron beam quality.

Since photoemission depends on the photon energy, $\hbar\omega$, and the electronic structure of the cathode material, an investigation to locate a resonance in one of the more efficient metal cathodes might be made to increase the quantum efficiency. Resonances are associated with the electronic shell structure of the cathode material. A resonant frequency for the incident photon energy could be found by varying the incident photon frequency with a tuned dye laser.

APPENDIX A

TABLE OF SYMBOLS AND ABBREVIATIONS

$\mathring{A}$	Angstroms (10^{-10} M)
E	Anode-cathode electric field (V/M)
V	Anode-cathode potential (Volts)
ArF	Argon Florine
I	Current (amps)
J	Current density (amps/cm^2)
DESY	Deutsches Elektronen Synchrotron
e.v.	Electron Volt
ν	Frequency of photon (Hertz)
Hz	Hertz (sec^{-1})
KrF	Krypton Florine
ϕ	Metal work function (electron Volts)
M	Meter
K	Perveance (amps/$Volt^{-1.5}$)
Z	Photocathode output (Volts)
$\hbar\omega$	Photon energy (electron Volts)
h	Planks constant (joule-sec)
P	Power per pulse (Watts/cm^2)
PHERMEX	Pulsed High-Energy Radiographic Machine Emitting X-Rays
η	Quantum efficiency (percent)
R	Resistance (Ohms)

APPENDIX B

LIST OF EQUIPMENT

Osciloscopes: Techtronics R-7103, 1GHZ
Vertical Base 7A29
Horizontal Time Base 7B15

DC Power Supply: Hipotronics Power

Laser: LAMBDA PHYSIK EMG 150T

Laser Variable Attenuator: NRC Model 935-10

High Vacuum Pump: CTI Cryogenics, Cryo-Torr-8

Photodiode: Hamamatsutu R1193U-04

Calorimeter: Gentec-200

Photodiode: EG and G Electronics FND-100Q

Photodiode Power Supply: BNC Portanim Model AP-3

Boxcar Averager: EG and G Princeton Applied Electronics Model 162

APPENDIX C

IMPROVED ANODE/COLLECTOR APPARATUS

Anode-Cathode Gap: 1.859 cm.

Cathode Spot Size: 1.797 cm^2 .

Restriction Aperture Area on Anode Face: 0.744 cm^2 .

Total Collector Area on the 50Ω Cable Face: 1.552 cm^2 .

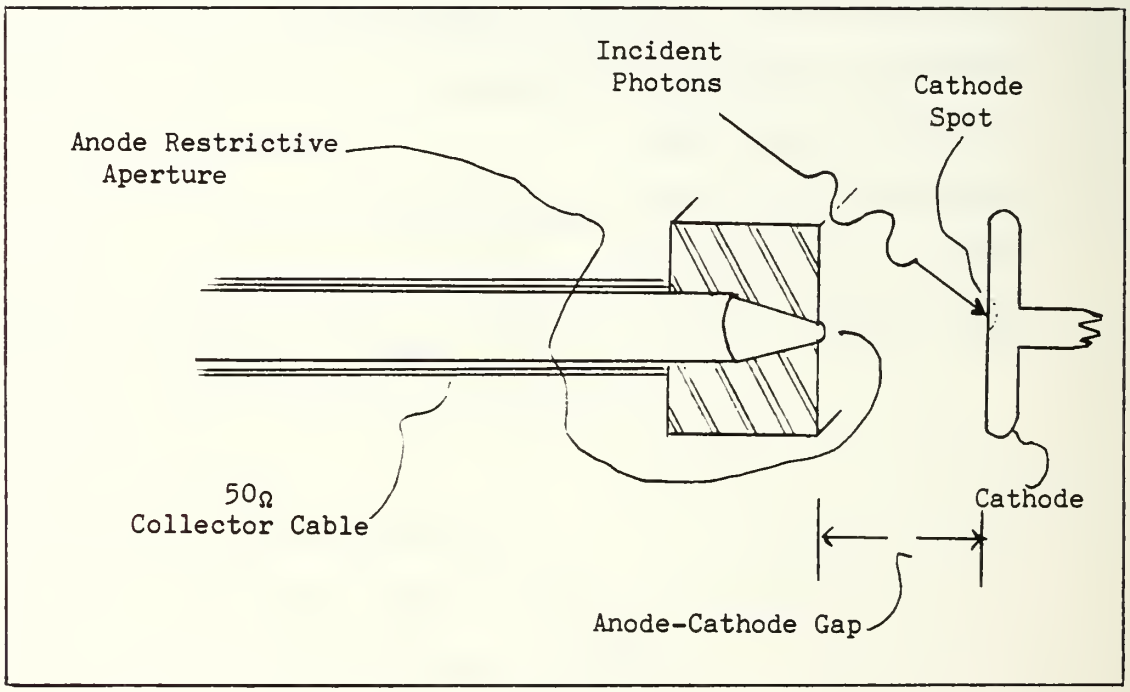

Figure 12. Improved Experimental Anode and Collector Geometry.

LIST OF REFERENCES

1. Lee, M. and Reifenberger, J. C., "Periodic Field Dependent Photocurrent from a Tungsten Field Emitter", Surface Science, v. 70, pp. 114-130, 25 April 1977.

2. Sommer, A. H., Photoemissive Materials, pp. 15, 19, 21-26, 33, 57-174, Robert E. Krieger Publishing Co., 1980.

3. Burroughs, E. G., "External Field Enhanced Photoemission in Silver-Cesium Oxygen Photocathodes", Applied Optics, v. 8, no. 2, pp. 261-265, February 1969.

4. Lee, C. H., Oettinger, P. E., Pugh, E. R., Klinkowsstein, R., Jacob, J. H., Fraser, J. S., and Sheffield, R. L., "Electron Emission of over 200 A/cm^2 from a Pulsed-Laser Irradiated Photocathode", IEEE Transcripts on Nuclear Science, v. 32, pp. 3045-3047, October 1985.

5. Walldeim, L., "Surface Photoelectric Effect for Thin Metal Overlays", Physics Letters, v. 54, pp. 943-946, 4 March 1985.

6. Bergland, C. N. and Spicer, W. E., "Photoemission Studies of Copper and Silver: Theory", Physics Review, v. 136, pp. 1030-1044, 16 November 1964.

7. Bergland, C. N. and Spicer, W. E., "Photoemission Studies of Copper and Silver: Experiment", Physics Review, v. 136, pp. 1044-1064, 16 November 1964.

8. Seitz, F., The Modern Theory of Solids, p. 139, McGraw Hill Book Co., 1940.

9. Feuerbacher, B., Fitton, B., and Willis, R. F., Photoemission and the Electronic Properties of Surfaces, pp. 3, 12, John Wiley and Sons, Inc., 1978.

10. Cardona, M. and Ley, L., Topics in Applied Physics: Photoemission in Solids I, v. 26, pp. 2, 21, 57, Springer-Verlag Co., 1978.

11. Gudat, W. and Kunz, C., "Close Similarity between Photoelectric Yield and Photoabsorption Spectra in the Soft-X-Ray Range", Physical Review Letters, v. 29, p. 170, 17 July 1972.

12. Barton, J. J., "Direct Surface Structure Determination with Photoelectric Diffraction", Physics Letters, v. 51, pp. 272-275, 25 July 1983.

13. Tredgold, R. H., Space Charge Conduction in Solids, pp. 70-71, Elsevier Publishing Co., 1966.

14. Naval Research Laboratory Memorandum Report 5853, Effects of Cathode Surface Roughness on the Quality of Electron Beams, by Y. Y. Lau, p. 4, 12 September 1986.

15. Hasted, J. B. and Phil, D., Physics of Atomic Collisions, 2nd ed., p. 171, Elsevier Publishing Co., 1972.

16. Downey, S. W., Builta, L. A., Moir, D. C., Ringler, T. J., and Saunders, J. D., "Simple Laser-Driven, Metal-Photocathode Electron Source", Applied Physics Letters, v. 49, pp. 911-913, 13 October 1986.

17. Palik, E. D., Academic Press Handbook Series: Handbook of Optical Constants of Solids, pp. 31-365, Academic Press, Inc., 1985.

18. Lawson, J. D., The Physics of Charged Particle Beams, pp. 172-177, Academic Press, Inc., 1958.

19. Sandia Laboratory Report SAND 84-0573, IIS: The Integrated TIGER Series Coupled Electron/Photon Monte Carlo Transport Codes, by J. A. Halbeib and T. A. Mehlhorn, 1984.

20. Saunders, J. D., Simple Laser-Driven, Metal Photocathodes as High Current Electron Sources, Master of Science Thesis, p. 29, Naval Postgraduate School, Monterey, California, December 1986.

21. Rudolf, H. W. and Steinmann, W., "Two Photon Photoelectric Effect in the Surface Plasma Resonance of Aluminum", Physics Letters, v. 61, pp. 471-472, 27 June 1977.

BIBLIOGRAPHY

Kittel, C., Introduction to Solid State Physics, 2nd ed., John Wiley and Sons, 1956.

Koller, L. R., The Physics of Electron Tubes, 2nd ed., McGraw-Hill Book Co., 1937.

Miller, R. B., An Introduction to the Physics of Intense Charged Particle Beams, Plenum Press, 1982.

Nagy, G. A. and Szilagyi, M., Introduction to the Theory of Space Charge Optics, Wiley Publishing, 1974.

Pierce, J. R., Theory and Design of Electron Beams, 2nd ed., D. Van Nostrand Co., 1954.

Zaidel, A. N. and Shreider, E. Y., Vacuum Ultraviolet Spectroscopy, Humphrey Science Publishers, 1970.

INITIAL DISTRIBUTION LIST

		No. Copies
1.	Defense Technical Information Center Cameron Station Alexandria, Virginia 22304-6145	2
2.	Library, Code 0142 Naval Postgraduate School Monterey, California 93943-5002	2
3.	Physics Library, Code 61 Department of Physics Naval Postgraduate School Monterey, California 93943	2
4.	Professor F.R. Buskirk, Code 61Bs Department of Physics Naval Postgraduate School Monterey, California 93943	2
5.	Professor J.R. Neighbours, Code 61Nb Department of Physics Naval Postgraduate School Monterey, California 93943	2
6.	Dr. D. C. Moir Hydrodynamics Group (M-4), P940 Los Alamos National Laboratory Los Alamos, New Mexico 87545	2
7.	LCDR Thomas J. Ringler, USN 337 Tuxford Place Fayetteville, North Carolina 28303	3

Thesis
R567
c.1

Ringler
Photocurrent generation from Basic metals, utilizing a short pulsed ArF excimer laser.